J. Iron Steel Res. Int. (2023) 30:875–886
https://doi.org/10.1007/s42243-023-00952-2

ORIGINAL PAPER

An online BOF terminal temperature control model based on big data learning

Jia-wei Guo[1] · Dong-ping Zhan[1] · Guo-cai Xu[2] · Nai-hui Yang[2] · Bo Wang[2] · Ming-xin Wang[2] · Geng-wei You[2]

Received: 2 January 2023 / Revised: 27 February 2023 / Accepted: 8 March 2023 / Published online: 20 April 2023

Abstract

The development of basic oxygen furnace (BOF) intelligent steelmaking model based on artificial intelligence and big data is the focus of international research and development. In the view of the current situation that the BOF cannot continuously detect the composition and molten steel temperature, combined with the monitoring results of the high-definition and high-brightness camera at the converter mouth, an online BOF terminal temperature control model is established based on big data learning case-based reasoning model and expert system model. The on-site online operation shows that the model can effectively improve the "flying lance" phenomenon and the splashing condition, the stability and safety of smelting process are better than that of artificial smelting, the "flying lance" rate decreases from 39.2% to 0, the early splashing rate decreases from 21.4% to 13.3% and the late splashing rate decreases from 81.25% to 56.7%. When the temperature fluctuation is controlled at ± 15 °C, the hit rate of the terminal temperature under the automatic control of the model is 90.91%.

Keywords Basic oxygen furnace · Case-based reasoning · Expert system · Steelmaking · Temperature

List of symbols

C_{lh}	Latent heat of hot metal melting, J/K
C_{lq}	Liquid heat capacity of hot metal, J/K
C_{sl}	Solid heat capacity of hot metal, J/K
$C_{sl'}$	Solid heat capacity of molten steel, J/K
$C_{lh'}$	Latent heat of molten steel melting, J/K
$C_{lq'}$	Liquid heat capacity of molten steel, J/K
C_j	Solid heat capacity of auxiliary materials, J/K
$f_{ss_{CaO}}$	CaO content in limestone, %
$f_{sh_{CaO}}$	CaO content in lime, %
$\overline{f}_{Si}$	Silicon content of sample hot metal, %
f_{Si}	Silicon content of hot metal, %
f_C	Carbon content of hot metal, %
L_{ss}	Limestone difference, kg
$\widehat{L}_{ss}$	Adjusted value of limestone based on alkalinity, kg
L_{Si}	Mass difference of hot metal silicon, kg
$\widehat{L}_{ss}$	Dolomite adjustment value, kg
$\overline{m}$	Sample hot metal mass, kg
m_{Fe}	Mass of hot metal, kg
m_{sb}	Sample dolomite addition amount, kg
m_{st}	Mass of scrap steel, kg
m_i	Mass of auxiliary materials, kg
m_j	Mass of preheated auxiliary materials, kg
m_k	Added mass of ore, kg
m_{ss_dl}	Limestone adjustment amount, kg
$\overline{m}_{sh}$	Lime adjustment amount, kg
n_{CO}	Ratio of CO in carbon–oxygen reaction, %
n_{CO_2}	Ratio of CO_2 in carbon–oxygen reaction, %
$pt_{Q_{Fe}}$	Physical thermal efficiency of hot metal, %
pt_C	Heat efficiency of carbon oxidation, %
pt_{Si}	Thermal efficiency of silicon oxidation, %
pt_i	Cooling capacity coefficient of scrap steel, %
Q_{Fe}	Physical heat of hot metal, J
Q_C	Heat of carbon oxidation, J
Q_{Si}	Heat of silicon oxidation, J
Q_{st}	Scrap steel absorbs heat, J
Q_{fl}	Heat absorption of auxiliary materials, J
Q_{yr}	Preheating heat of auxiliary materials, J
Q_{sy}	Surplus heat, J

✉ Dong-ping Zhan
zhandp1906@163.com

[1] School of Metallurgy, Northeastern University, Shenyang 110819, Liaoning, China

[2] Jianlong Acheng Iron & Steel Co., Ltd., Harbin 150000, Heilongjiang, China

Q_{CO} Thermal effect of CO, J/kg
Q_{CO_2} Thermal effect of CO_2, J/kg
Q_{SiO_2} Thermal effect of SiO_2, J/kg
Q_i Thermal effect of excipients, J/kg
Q_K Thermal effect of ore, J/kg
Q_{ss} Thermal effect of limestone, J/kg
Q_{sh} Thermal effect of lime, J/kg
R Sample final slag alkalinity
$\overline{R}$ Preset final slag alkalinity
T_r Melting point of hot metal, K
$T_{r'}$ Melting point of molten steel, K
T_0 Indoor temperature, K
T_{true} Hot metal temperature, K
T_{end} Molten steel temperature, K
T_{yr} Preheating temperature, K
Z_{MgO} Content of MgO in sample final slag, %
$\overline{Z}_{MgO}$ Preset MgO content in final slag, %

1 Introduction

Basic oxygen furnace (BOF) steelmaking is made of hot metal, scrap steel and ferroalloy as the main raw materials; without the aid of external energy, the process of steelmaking is completed in the BOF by the physical heat of hot metal itself and the chemical reaction between the components of hot metal. BOF steelmaking is one of the two major steel production processes in the world. The main purpose of BOF smelting is to achieve the target composition and molten steel temperature at the end of the blowing process [1], which requires the control of oxygen blowing mode and feeding mode within the smelting cycle [2], and the terminal temperature is related to the forward flow of the entire production and even affects the optimization of the production process [3]. Research and development of process control model based on the entire BOF steelmaking production process and smelting mechanism has become the core technology for the implementation of automatic control of BOF steelmaking [4]. At present, there are many prediction models about the end-point, and the commonly used prediction methods include the prediction method of state space model [5–7] and the prediction method based on historical data modelling [8–10]. Due to the lack of effective monitoring means of smelting process in traditional model, the "static control model" based on this model has not achieved good results.

With the rapid development of measurement technology, many new sensors and devices are put into use in the production process of BOF. Domestic and foreign scholars build corresponding models based on these devices and apply them to actual production, hoping to improve the control effect. Birk et al. [11] developed a real-time model and named it "dynamic control model" to distinguish it from "static control model". However, the "dynamic control model" is still based on physical and chemical laws. Because the BOF steelmaking process is accompanied by complex heat and mass transfer and chemical reactions, the "dynamic control model" is difficult to be reduced to a set of equations for modelling. In addition, the stability of the BOF process control directly affects the hit rate of the dynamic control model. The "dynamic control model" which only reflects the operation of the BOF through partial sensor results cannot adapt to the BOF smelting process under complex working conditions.

With the development of information technology, scholars have adopted artificial neural network (ANN) and other data-driven models to describe the mathematical relationship of smelting process. Due to its accurate identification of complex and nonlinear dynamic systems [12], ANN is suitable for modelling and controling in the process of steel manufacturing [13]. Radhakrishnan and Mohamed [14] used neural networks as soft sensors to predict the mass fraction of silicon and sulphur in blast furnace hot metal, and created an expert control system to improve the quality of hot metal. Pernía-Espinoza et al. [15] proposed several robust learning algorithms to train the neural network and described the annealing process of steel. For BOF steelmaking, Cox et al. [16] used ANN to predict oxygen and coolant requirements during the second blowing. Fileti et al. [17] developed an inverse neural network model to calculate the adjustment of oxygen blowing process at the end of smelting. Das et al. [18] used ANN with Bayesian regularization to predict the control behaviour of steelmaking process. Many successful applications of artificial neural network in steelmaking modelling have been studied in the literature. However, the ANN model is sensitive to initialization parameters, and it is difficult to adjust the structural parameters, which essentially affects the efficiency and prediction accuracy of ANN, and the ANN model is still difficult to meet the industrial requirements.

Jayadeva et al. [19] proposed a dual support vector machine (TSVM) algorithm in 2007. This method is an improved support vector machine algorithm to reduce the computational complexity of modelling and is widely used in classification applications. In 2010, Peng [20] proposed a dual support vector machine (TSVR) algorithm for regression, which can be used to build prediction models of industrial data. Based on the above modelling methods, various forecasting models in iron and steel production have sprung up. Brämming et al. [21] proposed tilt forecasting by using multivariate data analysis. Wang et al. [22] established a multilevel recursive regression model for predicting end-point phosphorus content in the BOF steelmaking process. Han and Liu [23] proposed an anti-

jamming end-point prediction model of extreme learning machine (ELM) based on evolutionary film algorithm. Wang et al. [24] proposed input weighted support vector machine modelling by applying input variable selection technique. Han and Cao [25] established a prediction model on the basis of improved case-based reasoning method. Scholars [26, 27] conducted a neural network prediction model to achieve the target endpoint conditions in molten steel. He and Zhang [28] developed a prediction model of terminal phosphorus content in BOF steelmaking process based on principal component analysis (PCA) and back-propagation (BP) neural networks. Gao et al. [29] developed a prediction model of BOF steelmaking end-point based on KNNWTSVR and LWOA. Zhou et al. [30] developed a prediction model of terminal phosphorus content of BOF based on monotone-constrained BP neural network. Qi et al. [31] developed a BOF end-point carbon prediction model based on real-time learning. Gao et al. [32] developed a wavelet transform weighted double support vector machine regression-based static terminal control for basic oxygen furnace steelmaking. Diaz [33] used infrared temperature measurement and prediction technology to predict the temperature of hot metal in basic oxygen BOF. These achievements are based on statistical and intelligent methods.

The end-point prediction model based on data learning has good guiding significance for BOF smelting, but it is difficult to be applied to actual control. There are essential differences between the actual control model and the prediction model. First, because the actual production requires excellent steel production conditions to be studied as the target, the data set of the actual control model is more stringent. Second, in order to meet the changes of actual production conditions, the actual control model needs stronger ability to adapt to the changes of process and raw material types, which is the lack of all models based solely on data learning. Third, the prediction model does not take into account the complex actual situation of the smelting state fluctuation, and the actual control model must consider the possible impact of the smelting state fluctuation on the final result. To sum up, the actual control model should not only be able to improve the accuracy of the model by data learning, but also be able to get rid of the dependence on the original data and adapt the solution to the process conditions.

The classical definition of case-based reasoning model (CBR) was proposed by Schank Ronger [34] in 1989. CBR uses existing experience to solve current problems and can well solve complex and changeable process conditions by combining mechanism analysis. Liang et al. [35] realized the prediction of terminal P content of BOF through attribute reduction two-step case-based reasoning. Gu et al. [36] used CBR model to predict endpoint carbon content of BOF. The CBR model can not only improve the model accuracy by relying on the big data learning method, but also put forward the modification of the solution by combining the mechanism model flexibly, which is suitable for the establishment of the online control model of BOF production.

In this paper, with Jianlong Steel 120 t BOF from as the research object, on the basis of auxiliary preheating process (temperature up to 500 °C), CBR model combined with metallurgical reaction mechanism is used to calculate the number of auxiliary materials, using expert system for static control of smelting process, stable process operation system. Combining the two methods, an online BOF terminal temperature control model based on big data learning was established to realize accurate control of the smelting process and terminal temperature of the BOF.

2 Production conditions

Jianlong Steel has a 120 t BOF, mainly producing Q195 and Q195C steels. In terms of classification, Q195 and Q195C steels belong to plain carbon steel with the same production process and little difference in terminal control objectives. The research object of the model in this paper is only Q195 and Q195C steels in normal smelting process, and the smelting condition under abnormal initial conditions is not discussed in this paper. The BOF is equipped with 4 high preheating silos. The main preheating raw materials include lime, limestone, dolomite and ore. The preheating temperature can reach 100–500 °C. In addition, the furnace mouth is equipped with high-resolution and high-brightness camera, through monitoring the light intensity of the furnace mouth to determine whether splashing occurs in the smelting process. At the end of smelting, the platinum–rhodium temperature probe was inserted into the melting pool of the converter by manually throwing to measure the temperature, some samples of molten steel were taken out, and the composition of molten steel was analysed quickly by the spectrometer.

3 System architecture

The structure of the online BOF terminal temperature control system is shown in Fig. 1. When smelting begins, the initial data are collected and transmitted to the CBR model. The case retrieval module transfers the case samples to the case adjustment module and expert system by matching and screening the case database data. The calculation results of expert system and case adjustment module are transmitted to object linking and embedding (OLE) for process control (OPC) platform at the same time.

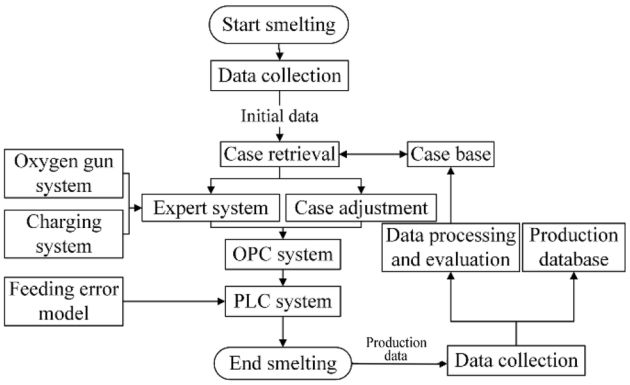

Fig. 1 Online BOF terminal temperature control system

The OPC platform controls the smelting equipment system with programmable logic controller (PLC). Due to the weighing deviation in the high bin of BOF, a feeding error model is developed to improve the weighing accuracy. After smelting, the production data enter the production database, and after cleaning and evaluation, it is selectively enters the case database to become new learning samples.

4 Establishment of terminal temperature model of online BOF

The online BOF terminal temperature control system mainly includes CBR model and expert system model. Among them, the CBR model is responsible for calculating the amount of raw material added under the current initial conditions. The expert system model is responsible for formulating the execution of the action flow of the oxygen lance and the feeding equipment.

4.1 Establishment of CBR model

CBR model can be regarded as a cycle of three steps: case retrieval, case adjustment and case learning. Among them, case retrieval is to screen out historical samples with attributes close to the current initial condition by formulating rules, and the effectiveness of case description in the case base is the fundamental guarantee for the success of the CBR model. Case adjustment can be divided into two situations. First, there is no difference in the type of attributes of the solution between the current case and the historical case, like the change of raw material type. In this case, mechanism model analysis or data regression prediction can be used to modify the solution. Second, there is a difference in the type of attributes between the current case and the historical case. In this case, the regression algorithm based on historical data will lose its function, and the solution can only be modified by means of mechanism model analysis. Case learning refers to the evaluation and learning of the solution satisfactory to the user and saving it in the case base. First of all, the case base is established.

4.1.1 Establishment of preferred case base based on historical big data

The case base is the starting point of CBR model operation. Before the formal operation of CBR model, the case base should be filled first. The database of common models can be divided into control model database and prediction model database. The case database of control model and prediction model has essential differences. In addition to cleaning the missing, discrete and other problem data of the initial data, the control case database also needs to make a judgement according to the production fluctuations monitored in the production process and the treatment of the end-point. Because case retrieval requires similar attributes, and the production process expects the end result to be superior, it requires that the case base of the control class model only stores the preferred sample. The samples with poor end-point control effect will not only occupy the retrieval resources, but also hardly be used by the retrieval. Three thousand production data were selected for optimization processing, and the results were put into the case database. The main rules of data screening are as follows:

(1) The optimal data must be complete in content, and accurate in value, and the value is a variable.
(2) In addition to the terminal composition and temperature meeting the process requirements, the optimal data should also meet the requirements of stable smelting process, no "flying lance" and serious splashing accident, no reblowing phenomenon, so as to ensure the safety of smelting.
(3) The technical index of the optimal data is better, the single consumption of molten iron is lower and the control interval of the terminal composition and temperature is narrower.

On the basis of satisfying the steel production process and data integrity, the process is screened, and the optimal data 420 groups are obtained. As the production process progresses, the case database will automatically filter the production data, and the preferred data that meet the requirements will be put into the case database to increase the number of preferred data.

Since the model in this paper is an online operation model, excessive feature items will affect the running speed of the model. In order to cooperate with the production process, it is necessary to reduce the number of feature items. Feature item screening is mainly divided by the influence of feature item on the solution through the

way of weight judgement. In essence, case analysis model is to analyse and calculate different cases with similar initial conditions. When the characteristic items of initial conditions fluctuate little between different cases, their influence on the solution will be very small. This makes it possible that feature items that are particularly important in mechanism calculations may not be important in case studies. For example, the content of Mn, P and S elements in hot metal and molten steel changes very little, and their influence on the change of terminal temperature is very weak.

The distribution of some feature items before and after screening is shown in Table 1.

4.1.2 Case retrieval

Case retrieval needs to quickly search for case samples with similar characteristics according to the initial conditions. The main feature items include hot metal composition, hot metal temperature, loading system and target molten steel temperature. Traditional case retrieval requires full-feature calculation and arrangement of all cases and current instances. When there are a large number of case base samples, this method requires a large amount of computing resources and cannot guarantee the retrieval speed. Based on the actual situation on site, this paper designs a retrieval method of step size indentation, as shown in Fig. 2. By comparing characteristic deviation values, this method gradually improves the case similarity, removes invalid samples and finally obtains the target samples.

4.1.3 Case adjustment

After obtaining the preferred sample through case retrieval, it is necessary to modify and adjust the case according to the current situation. The adjustment content includes the amount and type of auxiliary materials added. The CBR model uses the existing experience to model, so that the mechanism model only needs to calculate the adjustment of the case solution when the main features change. Because the preferred sample is similar to the current condition characteristic value, the calculation result changes from the traditional mechanism model to the calculation of the overall addition of characteristic value to the difference of the addition of characteristic value, reducing the calculation range of the mechanism model and narrowing the result deviation of the mechanism model.

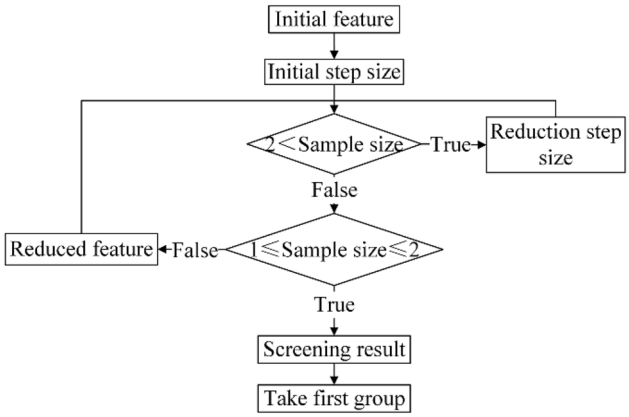

Fig. 2 Case retrieval rule

The purpose of the incremental calculation model of auxiliary materials is to meet the requirements of slagging and dephosphorization in the smelting process under the current initial conditions, and to calculate the amount of each auxiliary material. Because the case database data are similar to the characteristic value of the current furnace, the overall change of the amount of material added is small, and the quality of the BOF slag generated by default is the same. Based on the material balance, the heat increment model aims to reach the pre-set steel temperature by calculating the mass of iron-containing cold material or adjusting the amount and type of auxiliary materials. The main calculation formula [37] is shown in Table 2, the formula marked with * is derived by authors and the corresponding parameters are shown in summary table of symbols. Due to the reduction of the computational magnitude in the mechanism calculation process by the case analysis model, the calculation result is transformed from the overall addition calculation of eigenvalues by the traditional mechanism model to the difference addition calculation of eigenvalues, which makes the deviation calculation result of the mechanism model and the actual situation decrease simultaneously, and reduces the adverse influence of the calculation accuracy of the formula on the

Table 1 Case retrieval feature items

Characteristic item	Carbon content of hot metal/%	Silicon content of hot metal/%	Hot metal temperature/°C	Molten steel temperature/°C	Mass of hot metal/t	Mass of scrap steel/t
Pre-screening	3.0–7.3	0.2–1.8	1150–1450	1560–1680	70–95	10–25
Post-screening	3.7–5.7	0.2–0.75	1240–1410	1620–1670	84–96	6–18

Table 2 Case adjustment of main calculation formula

Calculation content	Equation	Serial number
Limestone difference	$L_{ss} = 2.14 \times R \times L_{Si}/f_{ss_{CaO}}$	(1)
Adjusted alkalinity value of limestone	$\widehat{L}_{ss} = 2.14 \times \overline{m} \times \overline{R} \times \overline{f}_{Si} - m_{Fe} \times R \times f_{Si} \times 1000/f_{ss_{CaO}}$	(2*)
Dolomite adjustment value	$\widehat{L}_{sb} = m_{sb} \times \left(\overline{Z}_{MgO} - Z_{MgO}\right)/Z_{MgO}$	(3*)
Physical heat of hot metal	$Q_{Fe} = pt_{Q_{Fe}} \times m_{Fe} \times \left(C_{sl}(T_r - T_0) + C_{lh} + C_{lq} \times (T_{true} - T_r)\right)$	(4*)
Hot metal carbon oxidation heat	$Q_C = pt_C \times m_{Fe} \times f_C \times (n_{CO} \times Q_{CO} + n_{CO_2} \times Q_{CO_2})$	(5)
Hot metal silicon oxidation heat	$Q_{Si} = pt_{Si} \times m_{Fe} \times f_{Si} \times Q_{SiO_2}$	(6)
Scrap steel absorbs heat	$Q_{st} = m_{st} \times pt_i \times \left(C_{sl'} \times (T_{r'} - T_0) + C_{lh'} + C_{lq'} \times (T_{end} - T_{r'})\right)$	(7*)
Heat absorption of auxiliary materials	$Q_{fl} = Q_i \times m_i$	(8)
Preheating heat of auxiliary materials	$Q_{yr} = C_j \times m_j \times \left(T_{yr} - T_0\right)$	(9)
Added mass of ore	$m_k = Q_{sy}/Q_K$	(10)
Limestone adjustment amount	$m_{ss\_dl} = Q_{sy}/(Q_{sh} \times f_{ss_{CaO}}/f_{sh_{CaO}} - Q_{ss})$	(11*)
Lime adjustment amount	$\overline{m}_{sh} = -m_{ss\_dl} \times f_{ss_{CaO}}/f_{sh_{CaO}}$	(12*)

results. Through the actual production process verification, the calculation accuracy meets the field requirements.

4.2 Establishment of expert system model

The control process of oxygen lance and charging affects the temperature of molten pool and the reaction rate of decarbonization in the smelting process, thus affecting the smooth progress of the production process and the control effect of the terminal temperature. Jianlong Steel adopts dry dust removal. Within 5 min of oxygen blowing, the system automatically monitors the concentration of CO and O_2 at the dust removal fan. When both concentrations reach 5% at the same time, an alarm will be triggered, resulting in "flying lance". The high occurrence period of "flying lance" accidents occurred during smelting 200–400 s. Splashing mainly occurs when smelting 200–400 s and 600–900 s. Under the shooting of the high-definition and high-brightness camera, it can be seen that the furnace mouth brightness caused by splashing or slag splashing rapidly increases to form two more concentrated peaks. The historical data of artificial smelting in 113 groups were randomly selected for analysis, and it was found that the rate of "flying lance" was as high as 39.2%, the splashing rate in the early stage was 21.4% and the splashing rate in the later stage was 81.25%.

4.2.1 Oxygen lance expert system model

In order to solve the problem of "flying lance" and splashing caused by artificial smelting, this paper mainly formulates the standard of oxygen lance action by "ignition period", "slagging period" and "carbon drawing period".

(1) "Ignition period"

The ignition process of BOF is not smooth, and the insufficient combustion of carbon elements in hot metal produces a large number of carbon monoxide and unburned oxygen into the dust removal fan, which is an important cause of the "flying lance" problem. In view of this phenomenon, the height of the oxygen lance is gradually reduced in the early stage of blowing, and the oxygen flow rate is gradually increased. The oxygen supply intensity is 10,000 m^3/h, the oxygen lance height is 2.3 m and blowing time is 20 s. The concentration of CO and O_2 is monitored at the dust removal fan. If CO concentration is greater than 3.5% and O_2 concentration is greater than 5%, oxygen flow rate decreases 4000 m^3/h and the lance position remains unchanged. Otherwise, oxygen supply intensity rises to 14,000 m^3/h, lance level drops to 2.1 m, after blowing for 15 s; oxygen supply intensity rises to 16,000 m^3/h, lance level drops to 1.9 m, with blowing time of 30 s. Keep monitoring CO and O_2 concentration until O_2 concentration $< 5\%$, ignition is successful, lance position gradually drops to basic lance position 1.5 m and oxygen flow gradually rises to 21,000 m^3/h.

(2) "Slagging period"

Smelting 90–240 s in slagging stage, the first batch of auxiliary materials forms alkaline slag with good fluidity, and the reaction stage of silicon manganese begins. At this point, the lance position is maintained at 1.5 m, and the flow rate is maintained at 21,000 m^3/h, the sampling results of the furnace mouth high-clearance and high-brightness camera are analysed continuously, if the furnace mouth light intensity exceeds 300 cd and lasts for more than 20 s,

the system determines that slag overflow or splashing occurs in the furnace, the lance height is adjusted to rise by 10 cm and the flow rate is reduced by 2000 m^3/h for 30 s. Smelting 240–360 s in the carbon–oxygen reaction stage, when CO concentration is greater than 20%, a large amount of CO and CO_2 gas may break through the slag layer and carry part of the slag to high altitudes causing splashing. During this period, the oxygen flow rate was reduced to 19,000 m^3/h, which eased the severity of the carbon–oxygen reaction.

(3) "Carbon drawing period"

After 780-s smelting, the carbon pulling stage was entered, and the CO concentration was less than 20%. The lance position is lowered to 1.3 m, and the flow rate is raised to 22,000 m^3/h for carbon drawing operation.

4.2.2 Feeding expert system model

The feeding expert system includes two parts: adding slagging materials and adding cold materials. The addition of slagging materials should ensure the effect of slagging and dephosphorization in the early stage, and arrange the addition number of auxiliary materials in each batch according to the furnace condition process. The addition of cold material should reduce the probability of splashing and ensure the stability of furnace condition.

(1) Adding slagging materials

The first batch of slagging materials is dolomite and limestone. In order to ensure the early-stage alkalinity and rapid slag-making requirements, the proportion of the first batch of auxiliary materials is required to account for 2/3 of the total added amount, and the added time is smelting for 90 s. The second batch of slagging materials will have an impact on the surface of the molten pool after being put into the BOF. If the mass of slagging materials is greater than 2 t for a single time, the auxiliary materials will throw the slag with low viscosity to the furnace mouth, resulting in slag overflow or splashing. In order to prevent this kind of situation, the second batch of auxiliary materials is added twice, each time accounting for 1/6 of the total amount and feeding time is smelting for 240 s.

(2) Adding cold materials

In the later stage of smelting, it is necessary to add iron-bearing cold material to adjust the temperature according to the heat condition of hot metal and the requirement of molten steel temperature. The single addition amount of cold material is less than 250 kg. The feeding time is 560 s for smelting, and the interval time is 50 s to prevent splashing caused by a large amount of FeO accumulated in the molten pool.

4.3 Establishment of feeding error model

Jianlong Steel uses vibration feeder to weigh auxiliary materials. The weighing speed and accuracy are affected by the frequency and time of aftershocks, so that it is difficult to give consideration to the weighing precision when the weighing speed is guaranteed. In order to prevent the total amount of various materials from exceeding the design value due to the accumulative error of a single weighing, the feeding error model is developed. The feeding error model monitors the written value of the material name before and after discharging in each silo, calculates and saves the difference between the actual discharging quantity and the designed discharging quantity and makes up the difference in the next stocking of the material in the silo; the calculated addition difference value is added with the next addition value of the auxiliary material. Because the weighing accuracy of the material scale is more than 150 kg, when the newly calculated number of auxiliary materials added is less than 150 kg, no action is performed.

5 Model implementation

This system uses Python to programme the charging and oxygen lance control system. OPC platform is used to control PLC equipment. Using SQL Server to design the underlying database, the OPC control platform integrates the control switch of blowing mode and feeding mode. During the production control process, the model can display information such as the position of oxygen gun and oxygen flow rate, which can help the model run smoothly.

6 Verification of running results of online temperature model

Through online BOF terminal temperature control model operation, 110 groups of production data were obtained for analysis, and carbon and phosphorus content of molten steel and steel temperature were obtained for verification. Among them, Q195 and Q195C steels require the terminal temperature to be 1630–1670 °C, carbon content of molten steel of 0.04%–0.10% and phosphorus content of molten steel $< 0.04\%$. The pre-set terminal temperature of the process, that is, the target control temperature of the model, is 1650 °C.

6.1 Result verification of components

The composition of molten steel is shown in Fig. 3. As shown from Fig. 3a, in the experimental results, the maximum carbon mass fraction of steel is 0.09%, the minimum is 0.05% and the average is 0.063%. As shown from Fig. 3b, in the experimental results, the maximum phosphorus mass fraction of steel is 0.04%, the minimum is 0.005%, the average is 0.022% and the average dephosphorization rate is 78.94%, meeting the process conditions.

6.2 Results of temperature verification

The molten steel temperature is shown in Fig. 4, in which the pre-set terminal temperature of CBR model is 1650 °C. As shown from Fig. 4, the highest, lowest and average molten steel temperature are 1669, 1630 and 1648 °C. The hit rate is 62.73%, 90.91% and 100% when the molten steel temperature fluctuation range is ± 10, ± 15 and ± 20 °C.

6.3 Validation of expert system control effect

Through the improvement of the oxygen lance operating system and charging system by the expert system, the smelting process is more stable, and some production parameters of BOF smelting are shown in Fig. 5.

By comparing Fig. 5a and d and Fig. 5b and e, it can be seen that the overall control effect of the oxygen lance basically reaches the design goal of the oxygen lance expert system, and the "flying lance" accident caused by the unsmooth ignition process is eliminated during the smelting period of 200–400 s. By comparing Fig. 5c and f, it can be seen that the peak of light intensity between 200 and 400 s during smelting shrinks significantly, the splashing rate in the early smelting stage drops to 13.3%, the peak of light intensity between 600 and 800 s during smelting shrinks and decreases overall and the splashing rate in the late smelting stage drops to 56.7%.

7 Analysis and discussion

Under the conditions of BOF production, many factors, such as temperature and composition fluctuation of hot metal, unknown amount and temperature of hot metal slag, variation of cooling capacity of scrap steel and uneven preheating of auxiliary materials, will have a certain impact on the accuracy of the model. The main impact analysis is as follows:

(1) Composition and temperature fluctuation of hot metal

The influence of the temperature fluctuation, carbon content and silicon content on the heat of hot metal can be obtained by using Table 2, Eqs. (4), (5) and (6), respectively. The calculation formula of the affected heat of hot metal on the change of terminal temperature ΔT is shown in Eq. (13).

$$T = Q_{\mathrm{dv}}/[(m_{\mathrm{Fe}} + m_{\mathrm{st}}) \times C_{\mathrm{lq'}} \times pt_{\mathrm{st}} + m_{\mathrm{sl}} \times C_{\mathrm{sl}})] \tag{13}$$

where T is temperature change of molten steel, K; Q_{dv} is caloric deviation value, J; pt_{st} is the yield of molten steel, %; and m_{sl} is quality of slag, kg.

Figure 6a shows the influence of hot metal component deviation on the terminal temperature. When the temperature of hot metal changes by 10 °C, the terminal temperature fluctuation of the model is 6.94 °C, and the maximum fluctuation at the theoretical is 9.2 °C. When the carbon component deviation of hot metal is 0.1%, the terminal temperature fluctuation of model is 12.3 °C, and the maximum temperature fluctuation of theoretical is 15.3 °C. When the deviation of silicon composition in hot

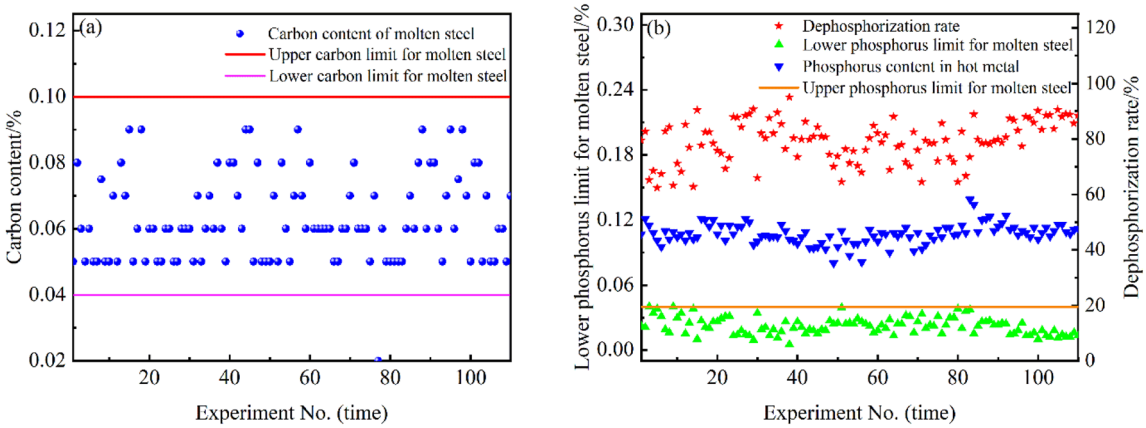

Fig. 3 Results of molten steel composition. **a** Test carbon mass fraction of molten steel; **b** dephosphorization effect of molten steel

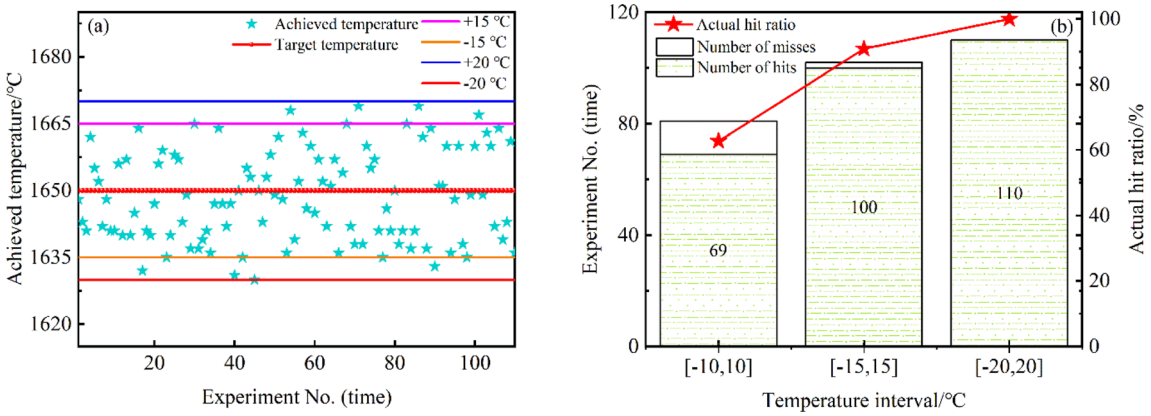

Fig. 4 Temperature control results of molten steel. **a** Temperature distribution of molten steel; **b** hit ratio of molten steel temperature

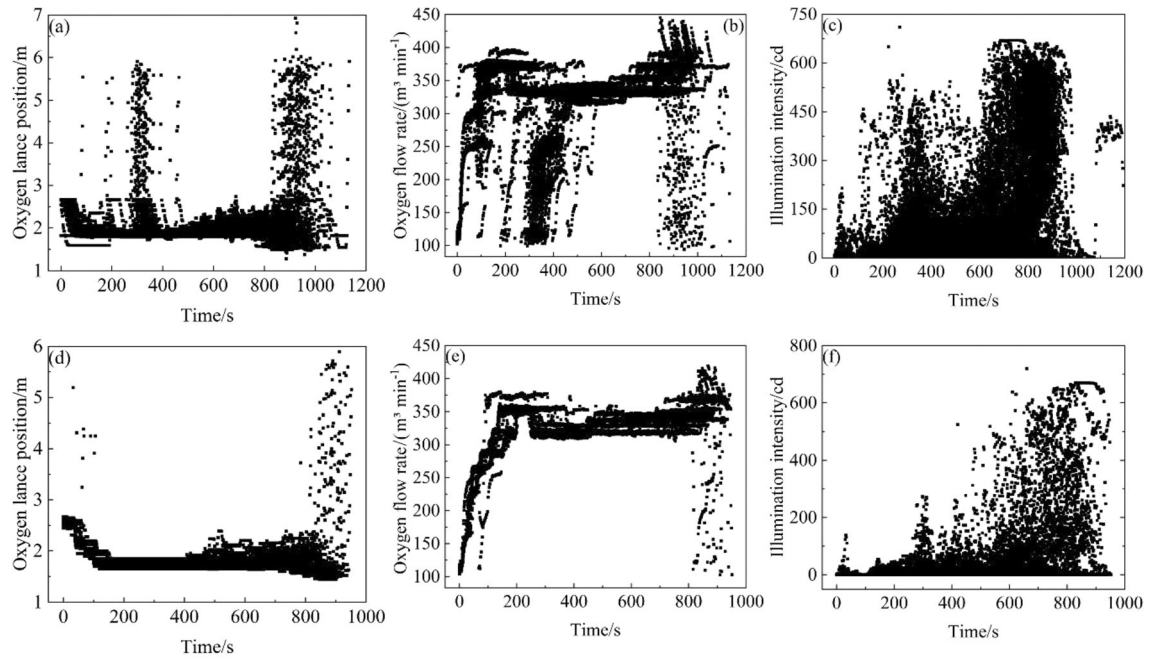

Fig. 5 BOF smelting process parameters. **a** Position of artificial smelting oxygen lance; **b** oxygen flow in artificial smelting; **c** artificial smelting light intensity; **d** position of system smelting oxygen lance; **e** oxygen flow in system smelting; **f** system smelting light intensity

metal is 0.05%, the terminal temperature fluctuation of the model is 12.86 °C, and the maximum temperature fluctuation at the theoretical is 16 °C. Because the deviation of hot metal silicon composition is more frequent in actual production, the deviation of hot metal silicon content has the greatest influence on the terminal temperature.

(2) Effect of slag quantity and temperature on blast furnace

The blast furnace slag enters the BOF along with the hot metal in the process of mixing iron. Part of hot metal heat is absorbed in the process of transforming blast furnace slag into BOF slag. The heat absorbed by blast furnace slag Q_{gsl} can be obtained by Eq. (14).

$$Q_{gsl} = m_{gls} \times C_{gsl} \times \left(T_{sl} - T_{gsl}\right) \tag{14}$$

where m_{gls} is the mass of blast furnace slag, kg; C_{gsl} is heat capacity of blast furnace slag, J/K; T_{sl} is temperature of the BOF slag, K; and T_{gsl} is the temperature of blast furnace slag, K.

By substituting the result of Eq. (14) into Eq. (13), the influence of blast furnace slag with different masses and temperatures on the final temperature can be obtained, as shown in Fig. 6b. It can be seen that the higher the mass of blast furnace slag, the lower the temperature and the higher the impact on the terminal temperature. When the mass of blast furnace slag is 3 t and the temperature is 1100 °C, the influence is the highest, which is 24.85 °C. When the mass

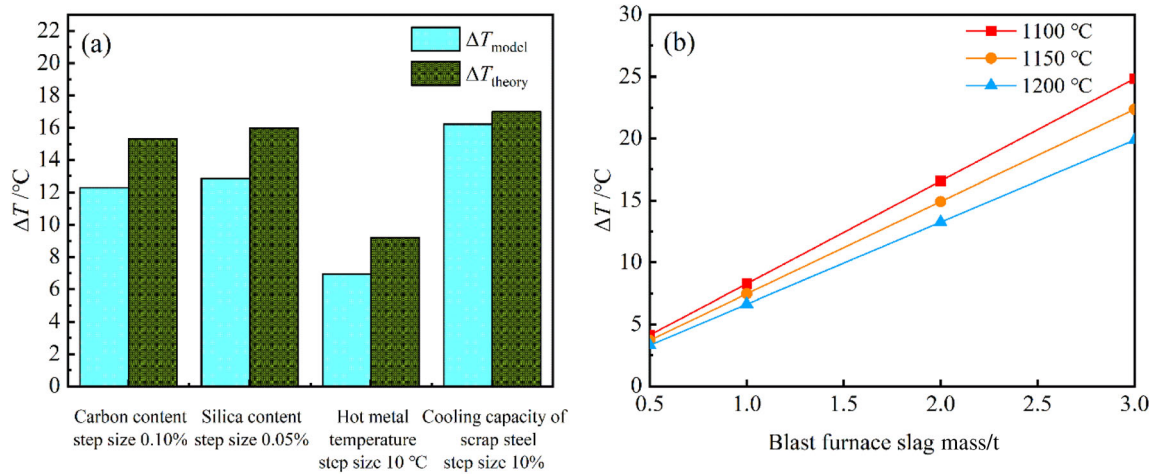

Fig. 6 Analysis diagram of influencing factors of terminal temperature. **a** Effect of hot metal and scrap on terminal temperature; **b** effect of blast furnace slag on terminal temperature

of blast furnace slag is 0.5 t and the temperature is 1200 °C, the influence is the lowest, which is 3.31 °C. However, in actual production, the slag carried by the iron ladle is usually only estimated by 3%–5%, which will affect the calculation accuracy of the model temperature.

(3) Scrap steel has not been classified and its composition is tested

Currently, iron and steel enterprises lack the capacity to classify and test scrap. Different types of scrap have different cooling capabilities. The calculation method of febrile element is the same as the influence method of the deviation of carbon and silicon in hot metal on the terminal temperature. The calculation process of heat absorption of scrap steel caused by different cooling capacity is shown in Eq. (7) (Table 2). By substituting the result of Eq. (7) with Eq. (13), the influence of scrap temperature dropping ability change on the terminal temperature can be obtained, as shown in Fig. 6a. When scrap cooling ability changes by 10%, the terminal temperature fluctuation of the model is 16.21 °C, and the maximum temperature fluctuation at the theoretical is 17 °C.

(4) Auxiliary materials are not preheated evenly

Jianlong Steel adopts hot blast furnace burning gas as heat source and transmits high temperature of 500–800 °C gas to the high silo at the top of the BOF to preheat the auxiliary materials into the furnace. Because the preheating temperature of auxiliary materials is not evenly distributed in the silo, the detected preheating temperature of the silo cannot reflect the whole preheating condition of the auxiliary materials. The influence of the preheating condition of auxiliary materials on the terminal temperature is shown in Fig. 7.

As shown from Fig. 7, if the deviation between the average preheating temperature and the detected preheating temperature increases by 100 °C, when the preheating mass of limestone is 6 t, the influence of terminal temperature can reach 3.78 °C. When the preheating mass of dolomite is 3 t, the influence of terminal temperature can reach 3.18 °C. When the preheating weight of lime is 3 t, the influence of terminal temperature can reach 1.56 °C. When the preheating mass of return ore is 2.5 t, the influence of terminal temperature can reach 4.75 °C. As the main auxiliary material in smelting process, limestone is used the most, and its preheating temperature test deviation has the greatest influence on the terminal temperature.

(5) Influence of other factors

Other factors that may lead to excessive drop in the temperature of the BOF lining, such as the shutdown of the BOF for maintenance and the delay of production due to the delay of production scheduling, cannot be measured quantitatively at present, but these factors will affect the molten steel temperature in the BOF and affect the accuracy of the temperature model.

8 Conclusions

1. This paper develops an online BOF terminal temperature control model based on big data learning CBR model and expert system model. By using the expert system to control the BOF smelting, the "flying lance rate" is reduced from 39.2% to 0, the early splashing rate is reduced from 21.4% to 13.3% and the late splashing rate is reduced from 81.25% to 56.7%. The smelting process controlled by model automation is

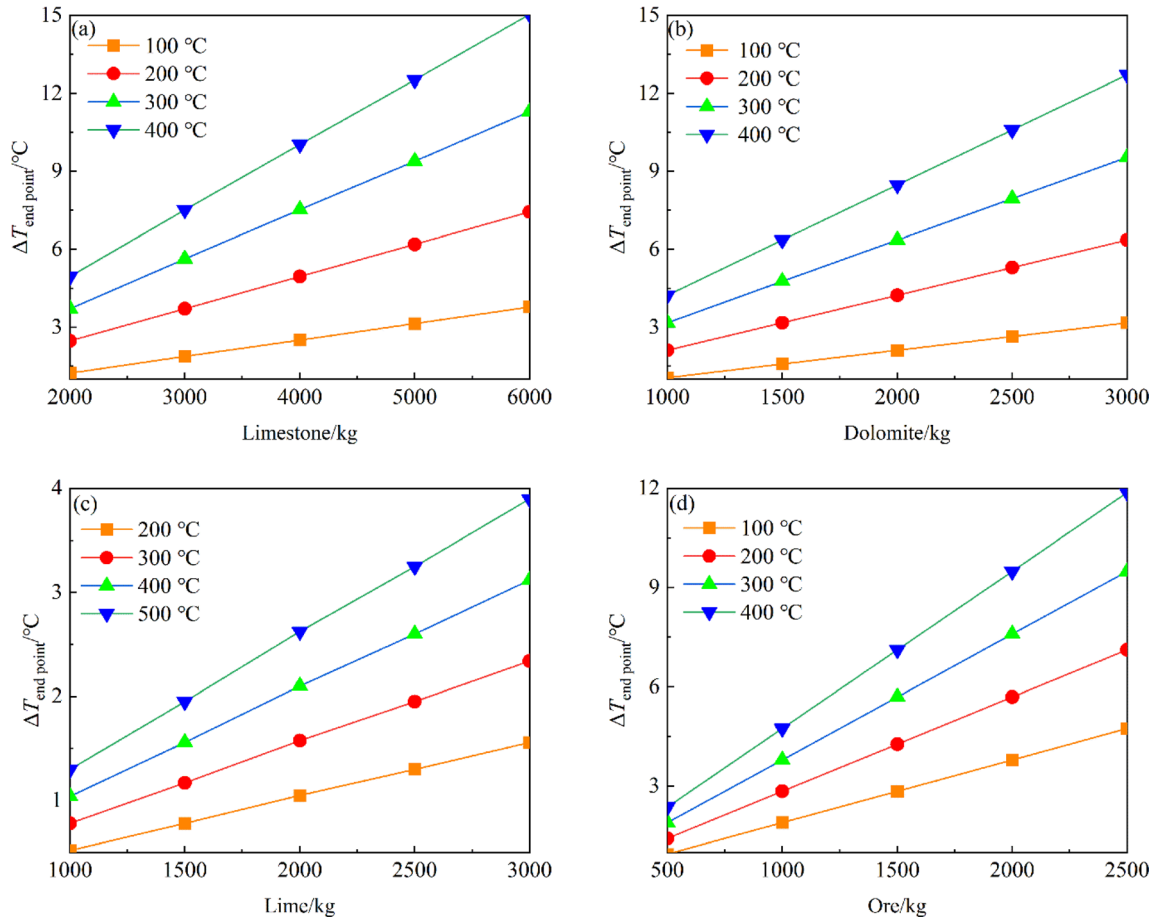

Fig. 7 Effect of preheating of auxiliary materials on terminal temperature. **a** Limestone; **b** dolomite; **c** lime; **d** ore

more stable than that of artificial smelting process, and the safety of smelting is also improved.

2. The pre-set terminal temperature of CBR model is 1650 °C. The maximum and minimum molten steel temperature is 1669 and 1630 °C, respectively, and the average molten steel temperature is 1648 °C. The hit rate is 62.73%, 90.91% and 100% when the molten steel temperature fluctuation range is ± 10, ± 15 and ± 20 °C, respectively.
3. The average carbon fraction and phosphorus fraction of molten steel in the model smelting furnace are 0.063% and 0.022%, respectively, and the average dephosphorization rate is 78.94%, which meet the actual process requirements.
4. The carbon, silicon and temperature deviation of hot metal have direct influence on the terminal temperature, and the silicon content deviation has the greatest influence under the same conditions. When the deviation of silicon composition in hot metal is 0.05%, the terminal temperature fluctuation of the model is 12.86 °C, and the maximum temperature fluctuation at the theoretical is 16 °C. The difference between the actual preheating temperature of auxiliary materials and the detected preheating temperature will affect the terminal temperature. The influence of limestone is the most obvious. When the temperature difference is increased by 100 °C and the amount of limestone is 6 t, the influence on the terminal temperature can reach 3.78 °C.

Acknowledgements The authors are grateful for the support from the Open Competition Scientific and Technological Research Projects of Heilongjiang Province (2022ZXJ03A02) and Jiangxi Provincial Technical Innovation Guidance Program (20202BDH80002).

Declaration

Conflict of interest We declare that we have no known competing financial interests or personal relationships that could have appeared to influence the work reported in this paper.

References

[1] R. Ding, L. Liu, Iron and Steel 32 (1997) No. 1, 22–26.
[2] W.L. Dong, Wisco Technology 1 (1990) 21–24+68.

[3] A.J. Xu, D.F. He, Z. Zheng, Fundamental textbook of metallurgical process engineering, Metallurgical Industry Press, Beijing, China, 2019.
[4] B. Du, China Metallurgy 12 (2002) No. 3, 32–34.
[5] M.T. Tham, G.A. Montague, A. Julian Morris, P.A. Lant, J. Process. Control 01 (1991) 3–14.
[6] H. Hapoglu, G. Özkan, M. Alpbaz, Chem. Eng. Commun. 183 (2000) 155–185.
[7] C. Gentric, F. Pla, J.P. Corriou, Comput. Chem. Eng. 21 (1997) S1043–S1048.
[8] K. Yamuna Rani, S.C. Patwardhan, Chem. Eng. Res. Des. 85 (2007) 1397–1406.
[9] B. Bakshi, Aiche J. 44 (1998) 1596–1610.
[10] Z.S. Hou, J.X. Xu, J. Automation 35 (2009) 650–667.
[11] W. Birk, A. Johansson, A. Medvedev, R. Johansson, IEEE Trans. Ind. Appl. 38 (2002) 565–570.
[12] L. Ching, T. Ching, Trans. Fuzzy Systems 8 (2000) 349–366.
[13] G. Bloch, F. Sirou, V. Eustache, P. Fatrez, IEEE Trans. Neural Networks 8 (1997) 910–918.
[14] V.R. Radhakrishnan, A.R. Mohamed, J. Process. Control 10 (2000) 509–524.
[15] A. Pernía-Espinoza, M. Castejón-Limas, A. González-Marcos, V. Lobato-Rubio, Ironmak. Steelmak. 32 (2005) 418–426.
[16] I.J. Cox, R.W. Lewis, R.S. Ransing, H. Laszczewski, G. Berni, J. Mater. Process. Technol. 120 (2002) 310–315.
[17] A.M.F. Fileti, T.A. Pacianotto, A.P. Cunha, Eng. Appl. Artificial Intelligence 19 (2006) 9–17.
[18] A. Das, J. Maiti, R.N. Banerjee, Expert Syst. Appl. 37 (2010) 1075–1085.
[19] Jayadeva, R. Khemchandani, S. Chandra, IEEE Trans. Pattern Anal. Mach. Intelligence 29 (2007) 905–910.
[20] X. Peng, Neural Netw. 23 (2010) 365–372.
[21] M. Brämming, B. Björkman, C. Samuelsson, Steel Res. Int. 87 (2016) 301–310.
[22] Z. Wang, F. Xie, B. Wang, Q. Liu, X. Lu, L. Hu, F. Cai, Steel Res. Int. 85 (2014) 599–606.
[23] M. Han, C. Liu, Appl. Soft Comput. 19 (2014) 430–437.
[24] X. Wang, M. Han, J. Wang, Eng. Appl. Artificial Intelligence 23 (2010) 1012–1018.
[25] M. Han, Z. Cao, Neurocomputing 149 (2015) 1245–1252.
[26] L.X. Kong, P.D. Hodgson, D.C. Collinson, ISIJ Int. 38 (1998) 1121–1129.
[27] J. Jiménez, J. Mochón, J.S. de Ayala, F. Obeso, ISIJ Int. 44 (2004) 573–580.
[28] F. He, L.Y. Zhang, Journal of Process Control 66 (2018) 51–58.
[29] C. Gao, M. Shen, X. Liu, L. Wang, M. Chen, Trans. Indian Inst. Met. 72 (2019) 257–270.
[30] K.X. Zhou, W.H. Lin, J.K. Sun, J.S. Zhang, D.Z. Zhang, X.M. Feng, Q. Liu, J. Iron Steel Res. Int. 29 (2022) 751–760.
[31] L. Qi, H. Liu, Q. Xiong, Z. Chen, Comput. Chem. Eng. 154 (2021) 107488.
[32] C. Gao, M. Shen, X. Liu, L. Wang, M. Chu, Complexity 2019 (2019) 1–16.
[33] J.L. Diaz, F.J. Fernandez, I. Suárez, Energies 12 (2019) 3235.
[34] C. Schank Roger, Dynamic memory: a theory of reminding and learning in computers and people, Cambridge University Press, New York, USA, 1983.
[35] Y. Liang, H. Wang, A.J. Xu, N.Y. Tian, ISIJ Int. 55 (2015) 1035–1043.
[36] M. Gu, A. Xu, H. Wang, Z. Wang, Processes 9 (2021) 1987.
[37] J.H. Feng, Design principle of steelmaking, Chemical Industry Press, Beijing, China, 2005.